Photodissociation dynamics of benzyl alcohol at 193 nm

Yuri A. Dyakov, Wen Hsin Hsu, Chi-Kung Ni, Wan-Chen Tsai, and Wei-Ping Hu

Additional information on J. Chem. Phys.

Photodissociation dynamics of benzyl alcohol at 193 nm

Yuri A. Dyakov,[1] Wen Hsin Hsu (許文馨),[1] Chi-Kung Ni (倪其焜),[1,a)]
Wan-Chen Tsai (蔡婉甄),[2] and Wei-Ping Hu (胡維平)[2,b)]
[1]*Institute of Atomic and Molecular Sciences, Academia Sinica, Taipei 10617, Taiwan*
[2]*Department of Chemistry and Biochemistry, National Chung Cheng University, Chia-Yi 621, Taiwan*

Photodissociation dynamics of benzyl alcohol, $C_6H_5CH_2OH$ and $C_6H_5CD_2OH$, in a molecular beam was investigated at 193 nm using multimass ion imaging techniques. Four dissociation channels were observed, including OH elimination and H_2O elimination from the ground electronic state, H atom elimination (from OH functional group), and CH_2OH elimination from the triplet state. The dissociation rate on the ground state was found to be 7.7×10^6 s^{-1}. Comparison to the potential energy surfaces from *ab initio* calculations, dissociation rate, and branching ratio from Rice–Ramsperger–Kassel–Marcus calculations were made. © *2012 American Institute of Physics*. [http://dx.doi.org/10.1063/1.4742935]

I. INTRODUCTION

Benzyl alcohol is the simplest aromatic alcohol. It is found in many plant products, foods, and is widely used in cosmetics and medication as a preservative and as a solvent in shampoos, lotions, perfumes, and sunscreens. The global production of benzyl alcohol is estimated to be about 100 thousand tons each year.[1] The release from cosmetics, shampoos, etc. has large impact on environmental chemistry.

Absorption spectrum of benzyl alcohol in the region longer than 230 nm has been reported.[2] An absorption band between 230 and 270 nm was observed. Neither the absorption spectra in the region shorter than 230 nm nor the assignment of the absorption spectra has been reported. Photodissociation of benzyl alcohol by IR multiphoton and UV photon at 193 nm has been studied using laser-induced fluorescence (LIF).[3,4] In UV photodissociation, OH and benzyl radicals were found to be the primary products. The nascent OH fragments probed by LIF showed that there is no significant population ($<2\%$) in the excited vibrational levels, but the initial rotational state distribution is Boltzmann-like, characterized by a rotational temperature about 1000 K. The translational temperature associated with OH was about 850 K. The benzyl radical was also monitored by LIF and found to be produced vibrationally hot. The measured rate constant for dissociation was found to be $(1.65 \pm 0.2) \times 10^6$ s^{-1}.

In this study, we report the photodissociation of benzyl alcohol $C_6H_5CH_2OH$ and $C_6H_5CD_2OH$, in a molecular beam at 193 nm using multimass ion imaging techniques. In addition to the OH elimination channel, the other dissociation channels were observed. The branching ratio, dissociation rate, and mechanism were reported. Comparison to the potential energies from *ab initio* calculations, dissociation rate, and branching ratios from the Rice–Ramsperger–Kassel–Marcus (RRKM) theory was made.

II. EXPERIMENT

The multimass ion imaging techniques have been described in detail in Refs. 5–7. Only a brief description is provided here. Benzyl alcohol vapor was formed by flowing ultrapure Ne at pressure of 250 Torr through a reservoir filled with benzyl alcohol sample at 25 °C. The benzyl alcohol/Ne mixture was then expanded through a 500 μm high temperature (60 °C) pulsed nozzle to form the molecular beam. Molecules in the molecular beam were irradiated by a 193 nm laser beam (20 ns pulse duration, Lambda Physik, Compex 200) and dissociated into neutral fragments. Due to recoil and center-of-mass velocities, the resulting fragments were distributed on an expanding sphere in flight to the ionization region. The fragments were subsequently ionized with a vacuum ultraviolet (VUV) (118 nm or 157 nm) laser pulse.

The distance and time delay between the VUV and photolysis laser pulses were set such that the VUV laser passed through the center of mass of the dissociation products and generated a line segment of photofragment ions by photoionization. The length of the segment was proportional to the fragment recoil velocity in the center-of-mass frame multiplied by the delay time between the photolysis and ionization laser pulses. To separate different masses within the ion segment, a pulsed electric field was used to extract the ions into a mass spectrometer after ionization. During mass analysis, the length of each fragment ion segment continued to expand in the original direction according to its recoil velocity. At the exit port of the mass spectrometer, a two-dimensional ion detector was used to detect ion positions and intensity distributions. In this two-dimensional detector, one direction represents the recoil velocity axis and the other direction the mass axis. The image of the ion intensity distribution for each mass-to-charge ratio generated from the photodissociation process described above is a line-shape image.

The ionization energy of benzyl alcohol is about 8.3 eV.[8,9] The energetic threshold of dissociative ionization $C_6H_5CH_2OH \rightarrow C_7H_7O^+$ (m/z = 107) + H was reported to be 10.03 eV by Russell *et al.*,[8] but it was found to be 10.46 eV

---

a)Also at Department of Chemistry, National Tsing Hua University, Hsinchu, Taiwan. Electronic mail: ckni@po.iams.sinica.edu.tw.
b)Electronic mail: chewph@ccu.edu.tw.

by Selim *et al.*[9] For the VUV laser set at 118.2 nm (10.5 eV), we found that benzyl alcohol cracks into smaller ionic fragments and produces background at m/z = 107 and 106. In addition, the ionization of fragments possessing low ionization potentials or large internal energies results in dissociative ionization and generated smaller ionic fragments. Ion images from dissociative ionization of parent molecules or fragments are both disk-like. However, the width of image from dissociative ionization of fragments change with the delay time, but the width of image from dissociative ionization of parent molecules does not change with the delay time. From the shape of the image and its change in width with delay time, images from the dissociation of neutral molecules and the respective dissociative ionization of neutral fragments can be distinguished.

The dissociation rate was obtained from the measurements of product growth and disk-like image intensity decay with respect to the delay time between the pump and probe laser pulses using time-of-flight mass spectrometer.

III. CALCULATION METHOD

Geometries and energies for reactant, products, and the corresponding transition states in the ground state and the first triplet state were calculated with the B3LYP/6-31G method.[10, 11] Energies of these structures then were refined by the G3(MP2,CCSD) scheme.[12, 13] All structure calculations were performed using the GAUSSIAN 03 package.[14] Calculations of dissociation rate coefficients for both singlet and triplet reaction channels were performed with our own code based on the RRKM theory.

The first three excited singlet state potential energy curves along O–H bond distance were calculated using the time-dependent (TD) density functional theory with the B3LYP functional and 6-311+G(d,p) basis set using the GAUSSIAN 03 package.

IV. RESULTS AND DISCUSSIONS

Fragments of m/z = 77, 79, 89, 91, and 105 were observed from the photodissociation of benzyl alcohol $C_6H_5CH_2OH$ at 193 nm using 118.2 nm VUV laser beam for ionization. Fragment m/z = 91 has large intensity, fragments m/z = 89, 79, and 77 have small intensities. The relative ion intensities are shown in the time-of-flight mass spectra in Figure 1. Photolysis laser intensities in the region of 0.89–15.8 mJ/cm^2 were used to determine the photon number dependence of these fragments. It shows that all photofragments result from one-photon dissociation. Fragment m/z = 105 was only barely observed in time-of-flight mass spectrometry. Ion image of m/z = 105 was strongly interfered by the cracking of parent ion, which produced strong signal at m/z = 107 and 106. It could not be observed in multimass ion image spectrometer using 118 nm photoionization. When VUV photon energy is changed to 7.9 eV (157 nm), fragment ions m/z = 79, 91, and 107 were observed. The ion image of m/z = 105 can be observed clearly without interference from the cracking of parent ions at this wavelength.
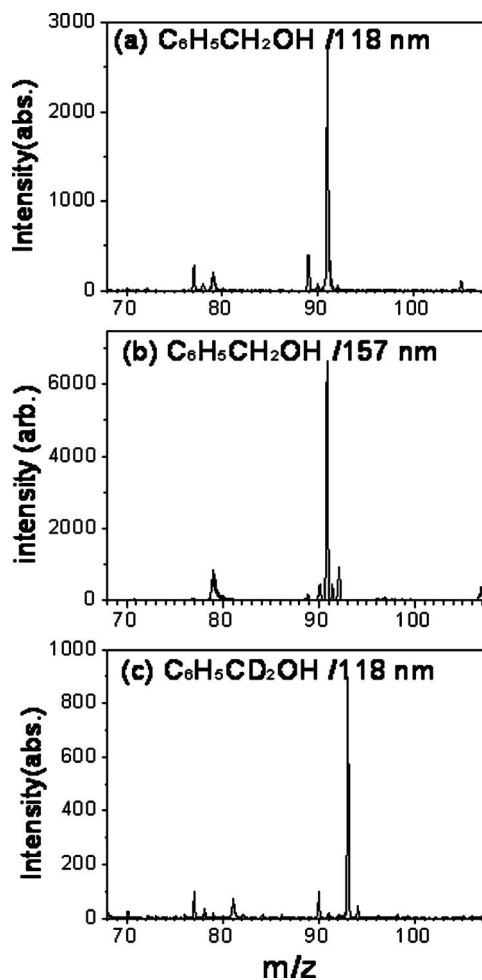
FIG. 1. Photofragment time-of-flight mass spectra from photodissociation of benzyl alcohol at 193 nm. (a) $C_6H_5CH_2OH$ using 118 nm photoionization, (b) $C_6H_5CH_2OH$ using 157 nm photoionization, (c) $C_6H_5CD_2OH$ using 118 nm photoionization. The backgrounds produced by 193 nm, 157 nm, and 118 nm have been subtracted.

A. OH elimination channel

Figure 2 depicts the photofragment ion images obtained from the photodissociation of benzyl alcohol at 193 nm using 118.2 nm VUV laser beam. Fragment m/z = 91 has a line shape image. It represents the fragment from OH elimination,

$$C_6H_5CH_2OH + h\nu\,(193\,nm) \rightarrow C_6H_5CH_2(m = 91) + OH. \tag{1}$$
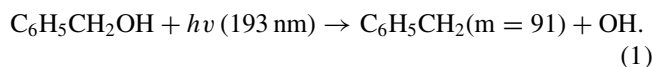
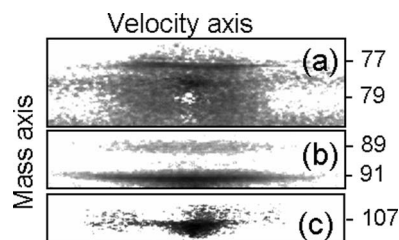The corresponding photofragment translational energy is shown in Figure 3.

FIG. 2. Photofragment ion imaging of m/z = 105, 91, 89, 79, and 77.
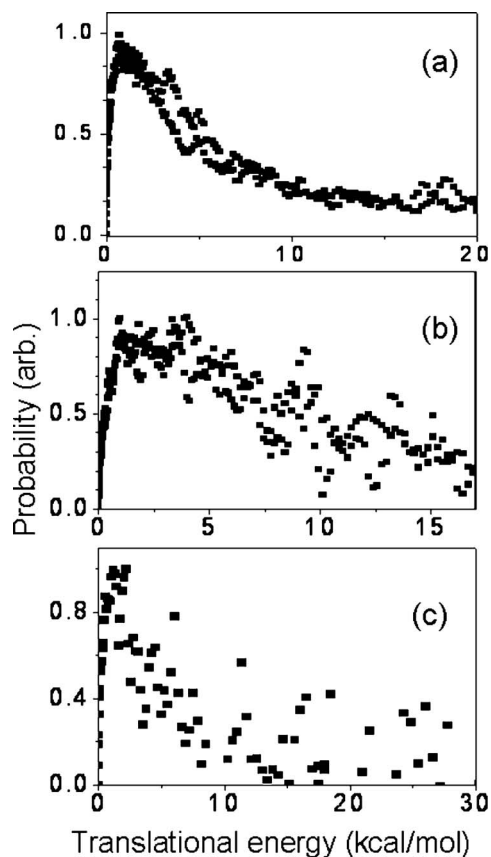
FIG. 3. Photofragment translational energy distribution of (a) reaction (1); (b) reaction (2); (c) reaction (4).

The geometries and energies of various transition states, and dissociation products in the ground electronic state from *ab initio* calculations are shown in Figure 4. Among various dissociation channels with loose transition states, OH elimination has the smallest dissociation threshold. This channel is
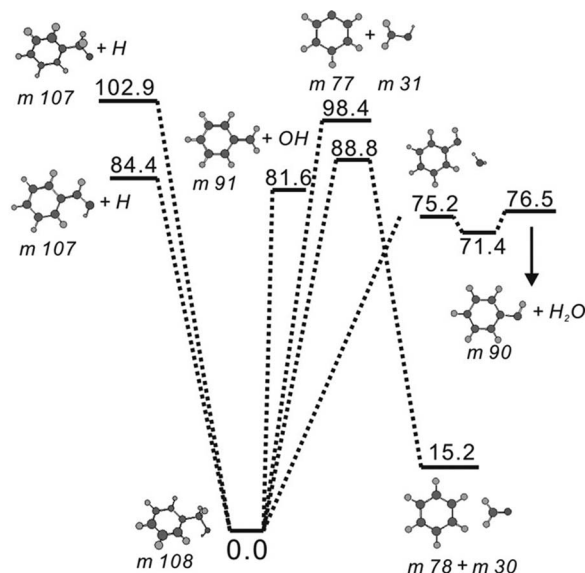

FIG. 4. Geometries and energies of various transition states, and dissociation products in the ground electronic state from *ab initio* calculations.
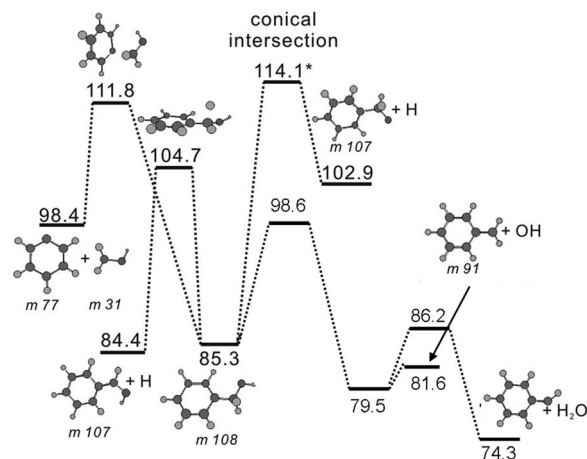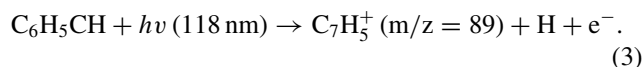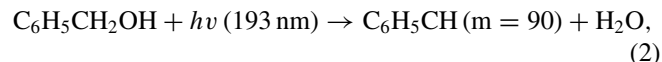

FIG. 5. Geometries and energies of various transition states, and dissociation products in the triplet electronic state from *ab initio* calculations.

expected to occur if excited benzyl alcohol undergoes internal conversion to the ground state.

We also explore the possibility that reaction occurs on the first triplet state. The geometries and energies of various transition states, and dissociation products in the first triplet state from *ab initio* calculations are illustrated in Figure 5. Although the OH elimination also has small dissociation threshold, it has a tight transition state and the exit barrier is as large as 17 kcal/mol. If OH elimination occurs on the triplet state, the photofragment translational energy release must be large. The small energy released in photofragment translational energy from experimental measurement suggests that OH elimination mainly occurs on the ground state. If it occurs on the triplet state, the relative branching ratio must be small and the corresponding signal is buried in the signal from the ground state dissociation.

B. H$_2$O elimination channel

Fragment m/z = 89 has a line shape image. It represents the fragment C$_6$H$_5$CH$_2$ produced from H$_2$O elimination, followed by the cracking upon VUV photoionization,

$$C_6H_5CH_2OH + h\nu\,(193\,nm) \rightarrow C_6H_5CH\,(m=90) + H_2O, \tag{2}$$

$$C_6H_5CH + h\nu\,(118\,nm) \rightarrow C_7H_5^+\,(m/z=89) + H + e^-. \tag{3}$$

Due to the large mass ratio between H and C$_7$H$_5^+$, the recoil velocity of C$_7$H$_5^+$ (m/z = 89) obtained from cracking (reaction (3)) is very small. Therefore, the velocity distribution of m/z = 89 is very similar to that of m = 90 and it does not change the image from line shape to disk-like by dissociative ionization in reaction (3).

H$_2$O elimination can occur easily on the ground state. It has the lowest dissociation barrier among all channels, as illustrated in Figure 4. The calculations also show that exit barrier of this channel is small, indicating that photofragment translational energy is small and the peak of the distribution
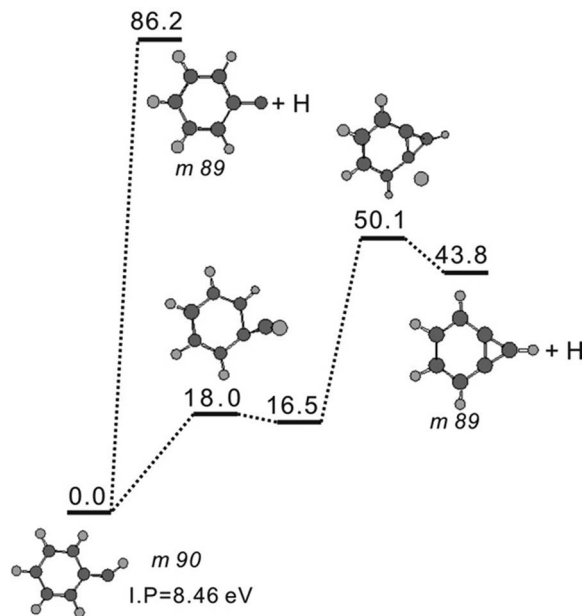
FIG. 6. Ionization potential of fragment C_6H_5CH (m = 90) and the dissociation channel of cation $C_6H_5CH^+$.

FIG. 7. Isomerization and dissociation of cations $C_6H_5CH_2O^+$ and $C_6H_5CHOH^+$.

must be very close to zero. This is consistent to the photofragment translational energy measurement, as shown in Figure 3.

The cracking of the fragment C_6H_5CH (m = 90) upon VUV photoionization is confirmed by *ab initio* calculations. Figure 6 shows that the adiabatic ionization potential is 8.46 eV. Following ionization, ion m/z = 90 cracks into smaller ionic fragment m/z = 89 through two pathways. One is the H elimination from the remaining H atom of CH_2OH functional group. The other is the H atom elimination from the aromatic ring. These two pathways have very different energetic thresholds. The former threshold energy is as large as 86 kcal/mol, such that 118 nm photon energy is not enough to overcome this barrier. On the other hand, the latter threshold energy is only 50 kcal/mol. The calculations suggest that H atom elimination must occur from aromatic ring due to the low dissociation threshold.

The cracking pathway described above was further confirmed by the experimental investigation of isotope substituted benzyl alcohol, $C_6H_5CD_2OH$. Following HDO elimination, one cracking channel is D atom loss from the α carbon atom, resulting in m/z = 89. The other cracking channel is H atom loss from the aromatic ring, resulting in m/z = 90. The experimental result, as illustrated in Figure 1(c), shows that the cracking channel is dominated by the H atom loss from aromatic ring. We also check the possibility of H_2O elimination on the triplet state. The calculations also show that H_2O elimination has large exit dissociation barrier on the triplet state. The small translational energy release in H_2O elimination from experimental measurement indicates that this channel does not occur on the triplet state.

C. H elimination channel

Fragment m/z = 79 has a disk-like image, as shown in Figure 2(a). It represents the fragment C_7H_7O produced from
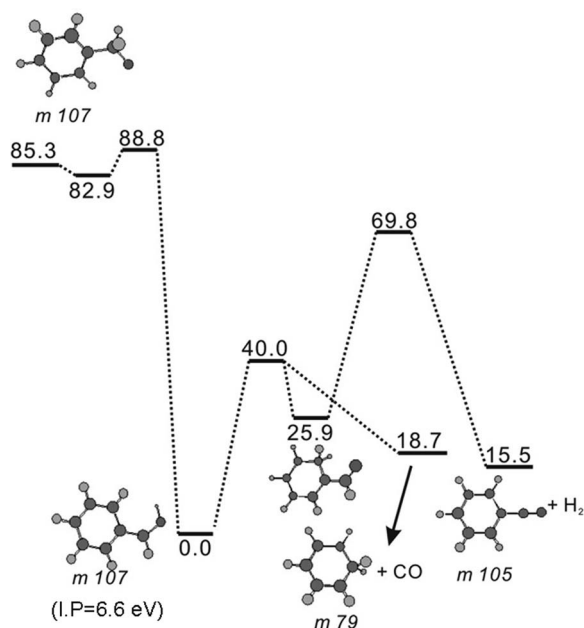
H elimination, followed by the cracking upon VUV photoionization,

$$C_6H_5CH_2OH + h\nu\,(193\,\text{nm}) \rightarrow C_7H_7O\,(\text{m} = 107) + H, \tag{4}$$

$$C_7H_7O + h\nu\,(118\,\text{nm}) \rightarrow C_6H_7^+\,(\text{m/z} = 79) + CO + e^-. \tag{5}$$
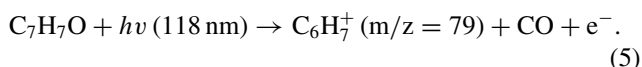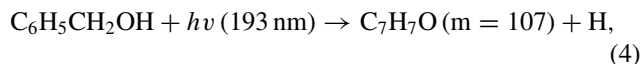
Figure 4 shows that H elimination from OH function group has much higher dissociation threshold than H atom elimination from the α carbon atom. If H atom elimination occurs on the ground state, H atom elimination must occur mainly from the α carbon atom. Following the H atom elimination from α carbon atom, fragment C_6H_5CHOH (m = 107) cracks into smaller ionic fragment, $C_6H_7^+$ (m/z = 79), due to its low ionization potential (ionization potential 6.6 eV), as illustrated in Figure 7.

On the other hand, the conical intersection between the first excited singlet state and the first triplet state occurs at the molecular geometry such that H atom elimination from OH function group can occur directly on the triplet state, as illustrated in Figure 5. Following the H atom elimination from OH functional group and then VUV photoionization, cation $C_6H_5CH_2O^+$ can isomerize to $C_6H_5CHOH^+$ easily, and then dissociates into smaller ionic fragment, $C_6H_7^+$ (m/z = 79), as shown in Figure 7.

The possibility of H atom elimination on the ground state or on the triplet state was further investigated by isotope substituted benzyl alcohol, $C_6H_5CD_2OH$. If D atom elimination occurs from the α carbon atom (which happens on the ground state), the ion produced after dissociative ionization (loss of CO) is m/z = 80. On the other hand, if H atom elimination occurs from the OH functional group (which happens on the triplet state), the ion after dissociative ionization (loss of CO) is m/z = 81. The experimental measurement shows that only H atom elimination from the OH functional group occurs, as
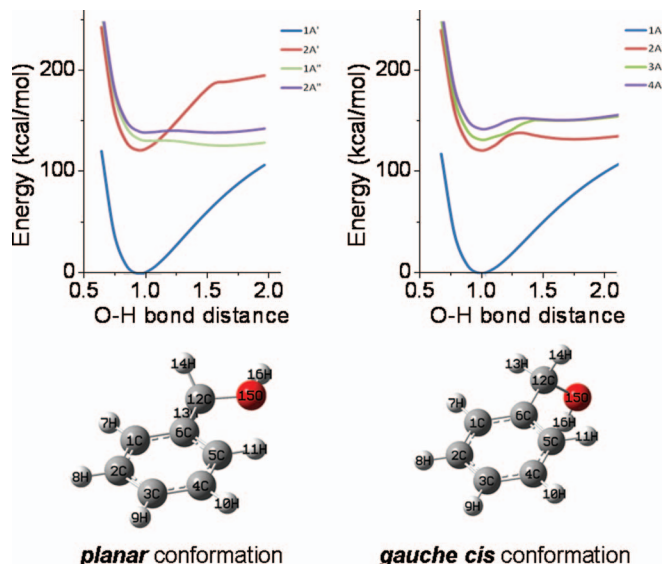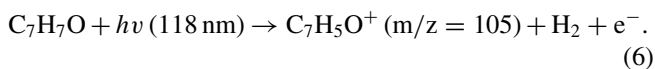
FIG. 8. First four singlet state potential curves along O–H bond distance of *planar* and *gauche cis* conformers.

shown in Figure 1(b). It suggests that H atom elimination occurs on the triplet state.

A small amount of m/z = 105 was observed. It represents the H atom elimination (reaction (4)), followed by the cracking upon VUV photoionization,

$$C_7H_7O + h\nu\,(118\,\text{nm}) \rightarrow C_7H_5O^+\,(m/z = 105) + H_2 + e^-. \tag{6}$$

The threshold of cracking upon ionization (reaction (6)), as shown in Figure 7, is low enough that it can occur at 118 nm photoionization.

The possibility of H atom elimination from the repulsive excited state along O–H bond distance was investigated from experimental measurement using different VUV photoionization energy. Figure 2(c) shows the ion image of fragment C_7H_7O (m = 107) from reaction (4). The VUV photon energy is changed to 7.9 eV such that no cracking occurs upon ionization. The corresponding photofragment translational energy is illustrated in Figure 3(c). It shows that only small amount of available energy is released in the translational energy. This is very different from the photofragment translational energy distribution of phenol[15] and hydroxybenzoic acid,[16] in which H atom elimination occurs on the repulsive potential energy surface along O–H bond distance. Large amount of available energy is released in the photofragment translational energy for these two molecules.

The possibility of H atom elimination from the repulsive excited state along O–H bond distance was also studied by *ab initio* calculations. The most stable geometry of benzyl alcohol calculated at the B3LYP/aug-cc-*p*VTZ level is *gauche cis* conformer. The rotation of CH_2OH along C–C bond results other stable conformers, including conformer with planar geometry (*Cs* symmetry). The energies relative to *gauche cis* conformer are within 1 kcal/mol. Figure 8 shows the ground state and the first three singlet excited states potential curves along O–H bond distance for

gauche cis and planar conformers. No repulsive potential curves along O–H bond distance similar to that of phenol[17] and hydroxylbenzoic acid[16] were found. Both experimental measurement and calculation results suggest that H atom elimination from the repulsive potential along O–H bond is negligible if not impossible.

D. CH₂OH elimination channel

Fragment m/z = 77 has a line shape image, representing fragment C_6H_5. It can result from the following dissociation:

$$C_6H_5CH_2OH + h\nu\,(193\,\text{nm}) \rightarrow C_6H_5 + CH_2OH. \tag{7}$$
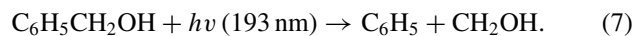
However, we did not observe ion CH_2OH^+. One possible explanation is that CH_2OH undergo secondary dissociation,

$$CH_2OH \rightarrow CH_2O + H. \tag{8}$$
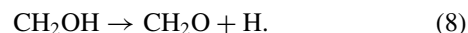
The ionization potential of the product CH_2O from secondary dissociation is too high (10.88 eV) (Ref. 18) to be reached by 118 nm photon energy and we are not able to detect it. The dissociation threshold of reaction (7) on the ground state is high, compared to the other channel. On the other hand, the corresponding threshold is not very high on the triplet state. It can compete with the other channels, as shown in the branching ratio calculations below. Therefore, it is likely that reaction (7) occurs on the triplet state.

E. Dissociation rate

The dissociation rate of the benzyl alcohol on the ground state due to 193 nm photon excitation was measured from the intensity changes of these disk-like images as well as from the product growths with respect to the delay time between pump and probe laser pulses. They are shown in Fig. 9. A dissociation rate of 7.7×10^6 s^{-1} was obtained from the fit of the experimental data to formula $A \times (1 - \exp(-k_1 t)) + B \times \exp(-k_1 t)$. The first term represents the product growth and the second term represents the decay of parent molecules. The dissociation rate from our measurement is about 5 times large than the value from the previous study,[4] but very similar to the dissociation rate of aromatic molecules with similar size, like toluene[19] and benzaldehyde.[20] The dissociation rate of the ground state calculated from RRKM
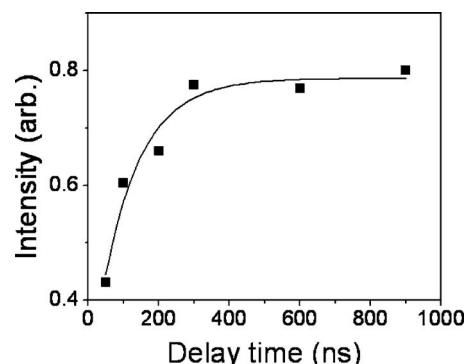

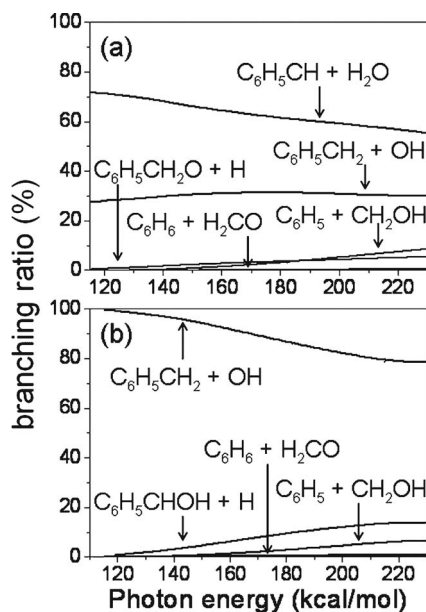FIG. 9. Product ($C_6H_5CH_2$) growth as a function of delay time between pump and probe laser pulse.

FIG. 10.   Branching ratios from calculations using RRKM theory. (a) Ground state; (b) Triplet state.

theory is 2×10^7 s^{-1}, which is very close to our experimental measurement.

The dissociation rate of the benzyl alcohol on the triplet state from the calculation of RRKM theory is 6×10^{10} s^{-1}. We have tried to measure the product growth as a function of delay time between pump and probe laser pulse delay time for ions m/z = 79, 77, which are the product of the triplet state. No change in these ion intensities was observed as a function of delay time. It is because the product growth is too fast to be observed by our instrument. We estimate the dissociation rate is larger than 1×10^8 s^{-1}, according to our instrument time resolution (20 ns). The dissociation rate measured from m/z. = 79 and 77 is different from the dissociation rate of the ground state. It confirms that m/z = 79 and 77 are produced from different electronic states.

F. Branching ratio

The relative branching ratio between reactions (1) and (7) can be estimated using the following argument. Photodissociation of toluene at 193 nm results in two dissociation channels: $C_6H_5CH_3 \rightarrow C_6H_5CH_2 + H$ and $C_6H_5CH_3 \rightarrow C_6H_5 + CH_3$.[21–27] The branching ratios were found to be 0.83 and 0.17, respectively.[23] We have studied the photodissociation of toluene at 193 nm using multimass ion imaging techniques.[19] The relative ion intensities of $C_6H_5CH_2^+$ and $C_6H_5^+$ from VUV photoionization at 118 nm were found to be 10:1. The relative ionization cross section at 118 nm between these two fragments can be calculated from the branching ratio and the relative ion intensities, 10/0.87:1/0.13 = 1.5:1 In the photodissociation of benzyl alcohol, the relative ion intensities of $C_6H_5CH_2^+$ and $C_6H_5^+$ from VUV photoionization at 118 nm are 9:1. The relative branching ratio for dissociation reaction (1) and reaction (7) therefore is 9/1.5:1/1 = 6:1. For the other fragments produced from benzyl alcohol, such as

m = 77, 79, 89, and 105, we do not have the relative ionization cross section at this wavelength. Therefore, we are not able to calculate the branching ratios of these channels. According to the relative branching ratio of reactions (1) and (7), the maximum branching ratio for OH elimination is 6/(1+6) = 86%.

The relative branching ratios from calculations using RRKM theory are illustrated in Figure 10. In the ground state, H_2O elimination is the major channel due to its low dissociation barrier. OH elimination is the second major channel. The rest of the others, such as H atom elimination and CH_2OH elimination are the minor dissociation channels. Two major dissociation channels from calculations are consistent with our experimental observation. On the other hand, calculations show that only OH elimination is the dominant channel on the triplet state. H atom and CH_2OH elimination channels are the minor channels in the triplet state. Two minor channels in the triplet state were observed experimentally. However, we did not observe the OH elimination on the triplet state. One possible explanation is that the amount of OH produced from the triplet state is small compared to the OH produced from the singlet state. They are not easy to be identified. This explanation also leads to the conclusion that most of the benzyl alcohol dissociate on the ground state, only small amount of them dissociate on the triplet state.

[1]Estimated from the major producers of benzyl alcohol, including Lanxess, Hubei Green Home Chemical, and Tessenderlo.
[2]J. Ghasemi, A. Niazia, and S. Ghobadi, J. Chin. Chem. Soc. **52**, 1049 (2005).
[3]P. K. Chowdhury, Ber. Bunsenges. Phys. Chem. **94**, 474 (1990).
[4]P. K. Chowdhury, J. Phys. Chem. **98**, 13112 (1994).
[5]S. T. Tsai, C. K. Lin, Y. T. Lee, and C. K. Ni, Rev. Sci. Instrum. **72**, 1963 (2001).
[6]C. K. Ni and Y. T. Lee, Int. Rev. Phys. Chem. **23**, 187 (2004).
[7]C. K. Ni, C. M. Tseng, M. F. Lin, and Y. Dyakov, J. Phys. Chem. B **111**, 12631 (2007).
[8]E. T. Selim, M. A. Rabbih, and M. A. Fahmey, Org. Mass Spectrom. **22**, 381 (1987).
[9]D. H. Russell, B. S. Freiser, E. H. McBay, and D. C. Canada, Org. Mass Spectrom. **18**, 474 (1983).
[10]A. D. Becke, J. Chem. Phys. **98**, 5648 (1993).
[11]C. Lee, W. Yang, and R. G. Parr, Phys. Rev. B **37**, 785 (1988).
[12]A. G. Baboul, L. A. Curtiss, P. C. Redfern, and K. Raghavachari, J. Chem. Phys. **110**, 7650 (1999).
[13]L. A. Curtiss, K. Raghavachari, P. C. Redfern, A. G. Baboul, and J. A. Pople, Chem. Phys. Lett. **314**, 101 (1999).
[14]M. J. Frisch, G. W. Trucks, H. B. Schlegel *et al.*, GAUSSIAN 03, Revision B.04, Gaussian, Inc., Pittsburgh, PA, 2003.
[15]C. M. Tseng, Y. T. Lee, and C. K. Ni, J. Chem. Phys. **121**, 2459 (2004).
[16]Y. L. Yang, Y. A. Dyakov, Y. T. Lee, C. K. Ni, Y. L. Sun, and W. P. Hu, J. Chem. Phys. **134**, 034314 (2011).
[17]A. L. Sobolewski, W. Domcke, C. Dedonder-Lardeux, and C. Jouvet, Phys. Chem. Chem. Phys. **4**, 1093 (2002).
[18]K. Ohno, K. Okamura, H. Yamakado, S. Hoshino, T. Takami, and M. Yamachi, J. Phys. Chem. **99**, 14247 (1995).
[19]C. K. Lin, C. L. Huang, J. C. Jiang, H. Chang, S. H. Lin, Y. T. Lee, and C. K. Ni, J. Am. Chem. Soc. **124**, 4068 (2002).

[20] A. Bagchi, Y. H. Huang, Z. F. Xu, P. Raghunath, Y. T. Lee, C. K. Ni, M. C. Lin, and Y. P. Lee, Chem-Asian J. **6**, 2961 (2011).

[21] H. Hippler, V. Schubert, J. Troe, and H. Wendelken, J. Chem. Phys. Lett. **84**, 253 (1981).

[22] J. Park, R. Bersohn, and I. Oref, J. Chem. Phys. **93**, 5700 (1990).

[23] R. Fröchtenicht, J. Chem. Phys. **102**, 4850 (1995).

[24] N. Nakashima and K. Yoshihara, J. Phys. Chem. **93**, 7763 (1989).

[25] K. Luther, J. Troe, and K. M. Weitzel, J. Phys. Chem. **94**, 6316 (1990).

[26] U. Brand, H. Hippler, L. Lindemann, and J. Troe, J. Phys. Chem. **94**, 6305 (1990).

[27] T. Shimada, Y. Ojima, N. Nakashima, Y. Izawa, and C. Yamanaka, J. Phys. Chem. **96**, 6298 (1992).